including electroencephalography (EEG), cerebral evoked potential, p300 event-related potential, psychometric hepatic encephalopathy score (PHES) and critical flicker test[7–15] have been employed. Diagnostic specificity can be improved by combining these tests, but complexity becomes a major disadvantage.

Recent advances in diagnostic imaging, such as positron emission tomography (PET) and functional magnetic resonance imaging (fMRI), made it possible to map brain function in tomographic images with high space and time resolutions. Recent study using PET[16] revealed that the primary event in the pathogenesis of OHE is inhibition of cerebral energy metabolism evidenced by reduced cerebral oxygen consumption and reduced cerebral blood flow. Whether the same mechanism could be applied to MHE is not known. Near-infrared spectroscopy (NIRS) is a tool that could non-invasively measure the cerebral blood volume as an oxygenated hemoglobin (oxy-Hb) concentration. The space and time resolution of NIRS is equivalent or higher than that of PET and fMRI. Moreover, NIRS is highly portable, does not have any restriction in the posture and flexible in setting tasks. Therefore it is possible to perform tests in a natural environment and to evaluate brain function as reflected by the dynamic changes in regional cerebral oxy-Hb concentration in response to a given task. The latter may be especially important to disclose a latent abnormality of brain function.

Recent study suggested that astrocytes regulate the cerebral blood flow and provide the oxy-Hb to the activation site of the brain.[17–19] In hepatic encephalopathy patients, function of astrocyte is impaired which may lead to cerebral oxygen consumption and blood flow.[16,20–22] We hypothesized that clinically latent abnormality of brain function in MHE also may be linked to the impairment of adequate increase in cerebral energy metabolism in response to the stimulation for activating the brain due to impaired function of astrocytes. In the present study, we used NIRS to evaluate the latent abnormality of brain function in patients with MHE, by measuring the increase of regional cerebral oxy-Hb concentration in response to task stimulation.

METHODS

Patients

A TOTAL OF 29 liver cirrhosis patients without OHE were enrolled. The underlying etiology of liver disease was hepatitis C virus infection in 19 patients, hepatitis B virus infection in two, alcoholic liver disease in five and other liver disease in three. All participants were examined by two psychiatrists to exclude mental disorders. No patient had any history of taking antidepressants or other psychotropic drugs. Subjects were examined by brain MRI or brain CT and they had no apparent brain structural disease including brain infarction. The study was performed in accordance with the Declaration of Helsinki and approved by the ethics committee of Musashino Red Cross Hospital and National Center of Neurology and Psychiatry. Informed consent was obtained from each subject. MHE was defined as those who had abnormal EEG findings. According to this definition, 16 patients were assigned to the MHE group and 13 were assigned to the non-MHE group. Table 1 shows the clinical characteristics of patients. The age and sex ratio did not differ between groups.

NIRS measurements

Concentration of oxy-Hb was measured by a 52-channel NIRS machine (Hitachi ETG4000; Hitachi Medical,

Table 1 Patient characteristics

	MHE ($n = 16$)	Non-MHE ($n = 13$)	*P*-value
Age	67.9 ± 8.9	70.1 ± 10.2	0.53
Sex (M/F)	7/9	7/6	0.72
Albumin (g/dL)	2.68 ± 0.39	3.63 ± 0.47	<0.0001
T-Bil (mg/dL)	1.83 ± 1.22	0.88 ± 0.34	0.011
PT%	64.5 ± 10.8	85.2 ± 12.7	<0.0001
Child–Pugh (A/B/C)	0/9/7	11/2/0	<0.0001
Etiology (HC/HB/Alc/Others)	8/2/4/2	11/0/1/1	0.28
NH3 (mmol/L)	90.1 ± 64.3	40.1 ± 18.3	0.012

Alc, alcoholic liver disease; HB, hepatitis B; HC, hepatitis C; MHE, minimal hepatic encephalopathy; PT%, prothrombin time percentage; T-Bil, total bilirubin.

Tokyo, Japan). NIRS detects changes in brain activity by capturing increases in regional cerebral blood flow caused by neural activity. For each channel, an optic fiber device is connected to an application probe that is placed on the subject's scalp. The 52 channels cover the frontal lobe, upper temporal lobe and anterior parietal lobe of the brain (Fig. 1). The near-infrared light penetrates the scalp and skull, passes through the brain tissue, and is partially absorbed by oxy-Hb. The reflected light is detected by a probe positioned 30 mm away from the application probe. The changes in concentration of oxy-Hb can be calculated by measuring reflected light.[23] In this study, the results measured by the seven channels which were previously reported to be diagnostic for mental disorders; (channels 36–38 and 46–49)[24–26] were selected for the analysis. The time-dependent changes in oxy-Hb concentration in each of these seven channels were compared between MHE and non-MHE patients. The sum of increase in oxy-Hb concentration in these seven channels was calculated and compared between MHE and non-MHE patients. For this analysis, increase of oxy-Hb at 5 s and maximum increase were used.

Activation task

A word-fluency task was used to stimulate frontal lobe activity. Subjects were instructed to generate as many words as possible with a given letter. For example, with a task involving "naming words starting with the letter 'T' ", subjects were given 20 s to say as many words as they could starting with the letter "T", such as "tomato", "tail" and "tea". Three tasks were presented for a total of 60 s. During the word-fluency test, the real-time changes in the oxy-Hb concentration were measured at each channel. Data are expressed as a wave form as well as in the form of topographic images.

Statistical analysis

The SPSS software package ver. 15.0 (SPSS, Chicago, IL, USA) was used for statistical analysis. Categorical data were analyzed using Fisher's exact test. Continuous variables were compared with Student's *t*-test. A *P*-value of less than 0.05 was considered statistically significant.

RESULTS

THE NUMBER OF words generated by the word-fluency task did not differ significantly between the MHE and non-MHE groups (10.8 ± 3.4 vs 10.7 ± 2.5 words, $P = 0.93$). Figure 2 shows the time-dependent changes in the oxy-Hb concentration during the task in the representative seven channels. The average value of the seven channels (36–38 and 46–49) is shown in Figure 2. These changes reflected frontal lobe activation by the word-fluency test and correspondingly elevated cerebral blood flow in the frontal lobe. In the non-MHE

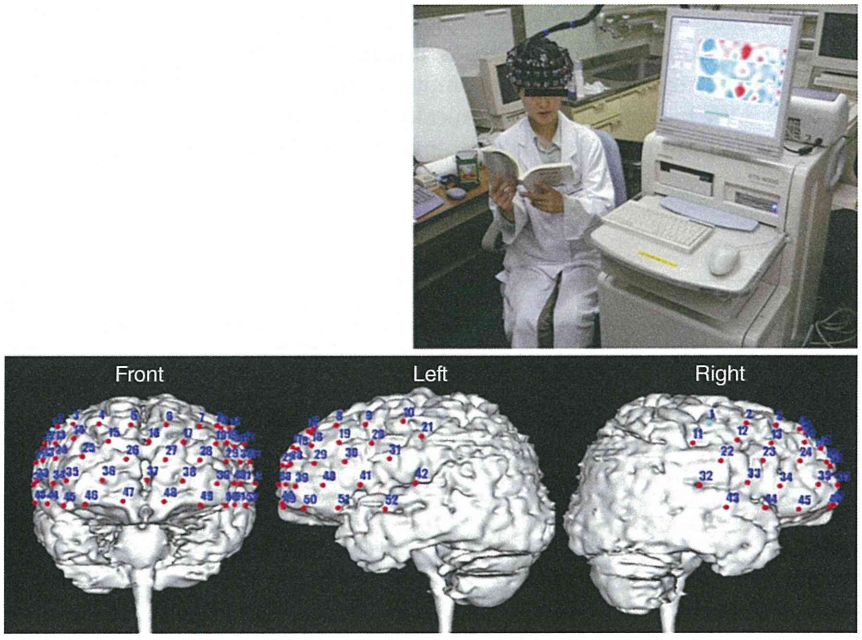

Figure 1 Near-infrared spectroscopy. An optic fiber device connected to a probe is placed on the subject's scalp covering the frontal to temporal regions. The relative concentration of oxygenated hemoglobin (oxy-Hb) was measured every 0.1 s during word-fluency testing.

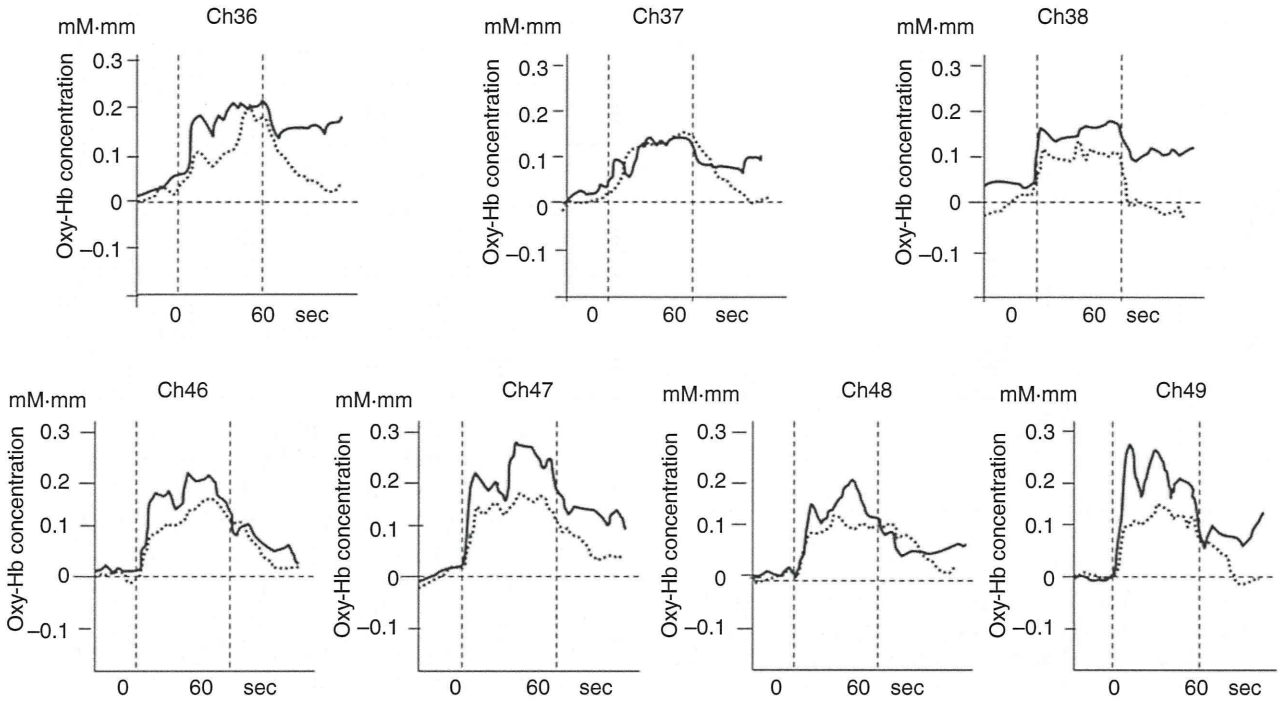

Figure 2 Time-dependent changes in oxygenated hemoglobin (oxy-Hb) concentration in response to tasks. The average waveforms of time-dependent changes in oxy-Hb concentration in representative channels (Ch) are shown. The solid and broken line represents non-minimal hepatic encephalopathy (MHE) and MHE groups, respectively. The area between the two vertical lines corresponds to the 60 s of the word-fluency test.

group, the oxy-Hb concentration increased immediately after the start of the task, remained high with repetitive steep peaks during the task, and decreased after the end of the task. In contrast, the time course of oxy-Hb changes was somewhat different in the MHE group, characterized by a slow increase of oxy-Hb throughout the task, gradually reaching a plateau at the end of the task (Fig. 2). These differences in the degree of oxy-Hb changes also could be visualized by the topographic presentation. In the topographic image, increase of oxy-Hb concentration is expressed as a deepening of the red shading. Figure 3 shows a topographic image showing the increase in oxy-Hb concentration in response to a task. The image in Figure 3 is the average value (arithmetic mean topographic image) of all patients. The concentration of oxy-Hb is small in the MHE group, as reflected by blue or green color, compared to the non-MHE group, as reflected by orange or red color.

When the average value of the seven channels were calculated, the maximum value of oxy-Hb increase was smaller in MHE compared to non-MHE patients but it did not reach statistical significance (0.26 ± 0.12 vs 0.32 ± 0.22 mM · mm, $P = 0.37$) (Fig. 4). On the other hand, increase in oxy-Hb concentration at 5 s after starting the task was significantly small in MHE compared to non-MHE patients (0.03 ± 0.05 vs

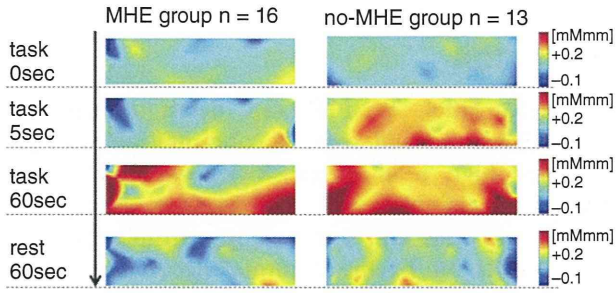

Figure 3 Topographic image showing cumulative increase in oxygenated hemoglobin (oxy-Hb) concentration. Increase in oxy-Hb concentration is shown by deepening of the red shading. The concentration of oxy-Hb is small in the minimal hepatic encephalopathy (MHE) group, as reflected by the blue or green color compared to the non-MHE group as reflected by orange or red color.

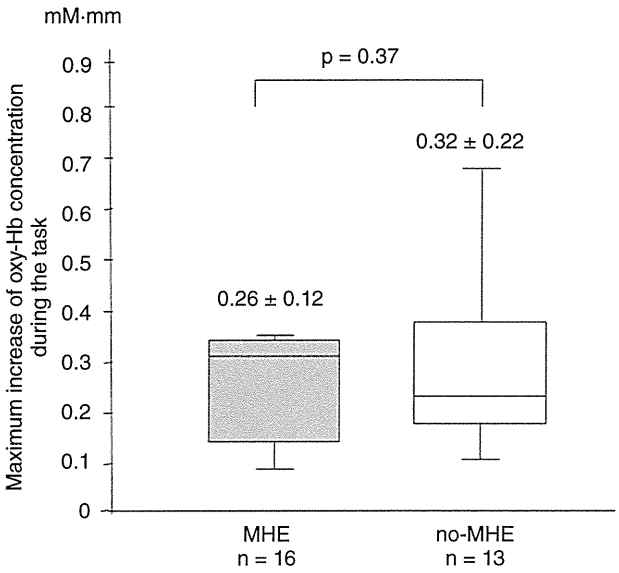

Figure 4 Comparison of maximum increase in oxygenated hemoglobin (oxy-Hb) concentration between patients with and without minimal hepatic encephalopathy (MHE). The average value of maximum increase in oxy-Hb did not differ significantly between the MHE and non-MHE groups.

0.11 ± 0.09 mM · mm, $P = 0.006$) (Fig. 5). For the diagnosis of MHE, the receiver–operator curve analysis identified an optimal cut-off of 0.05 mM · mm for the oxy-Hb concentration at 5 s after starting the task. The area under the curve was 0.774 ($P = 0.012$; 95% confidence interval, 0.60–0.95), sensitivity and specificity of NIRS for the diagnosis of MHE was 69% and 77%, respectively. The positive predictive value was 79% and negative predictive value was 67%.

DISCUSSION

USING NIRS, WHICH can detect changes in regional cerebral oxy-Hb concentration with an extremely high level of sensitivity, we found that increase in cerebral oxy-Hb concentration in response to tasks was slow and small among cirrhotic patients without OHE but having abnormal electroencephalography findings. The impairment of response was most significant at an early time point after the start of the task. These findings indicated that cerebral oxygen metabolism is poorly reactive in response to tasks among patients with MHE and that this impaired cerebral oxygen metabolism may be related to the pathogenesis of latent impairment of brain activity seen in MHE. To the best of our knowledge, our study appears to be the first evaluating MHE with NIRS. The non-invasiveness and high time resolution of NIRS give it potential as a valuable research tool for the examination of brain function in HE, as well as a clinically useful tool for the diagnosis of MHE.

Hepatic encephalopathy in its early stage, such as latent or minimal HE, can reduce cognitive function, lower work efficiency, reduce QOL[27,28] or impair driving skill.[1,2,29,30] Although there are several practical requirements for the diagnosis of MHE, adequate diagnosis of MHE is difficult due to the lack of reliable diagnostic standards.[31,32] Several diagnostic methods such as neuropsychological function tests, number connection test, light/sound reaction time, inhibitory control test, WAIS or electro-psychological tests including EEG, spectral EEG, and cerebral evoked potential, PHES, critical flicker test and computer-aided quantitative neuropsychological function test system (NP-test)[7–15] have been proposed,[32–36] but there is no ideal test for MHE as yet. Because these tests are developed for the screening of MHE, these are not diagnostic. Establishment of a reliable diagnostic method for MHE is imperative. We

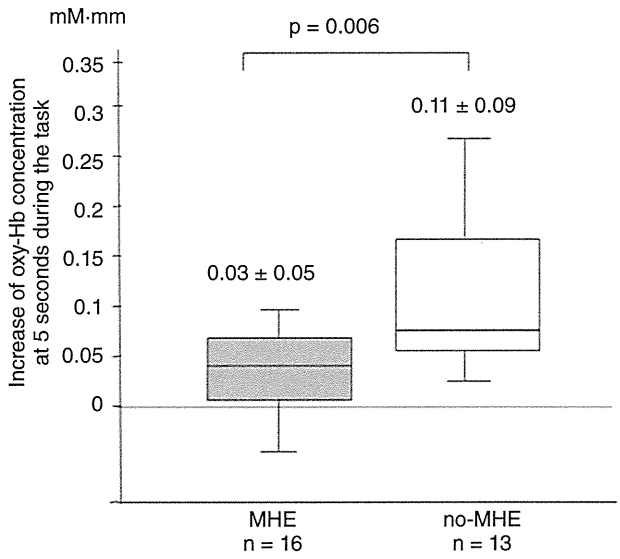

Figure 5 Comparison of increase in oxygenated hemoglobin (oxy-Hb) concentration at 5 s after the start of task between patients with and without minimal hepatic encephalopathy (MHE). The average value of increase in oxy-Hb was compared between the MHE and non-MHE groups at 5 s after starting the word-fluency task. The increase in the oxy-Hb concentration was significantly lower in patients with MHE compared to non-MHE ($P = 0.006$).

have some cases in which NIRS results improved with lactulose and branched-chain amino acid. A prospective study is ongoing to evaluate the effect of treatment by NIRS. The major advantage of NIRS over "paper and pencil tests" is the absence of learning effect which is generally seen in other neuropsychological function tests[37] and NIRS could also discriminate other mental disorders.[24,25]

Neuroimaging using MRI, magnetic resonance spectroscopy and PET has made it possible to non-invasively assess hepatic encephalopathy.[38–47] However, these tests require extensive equipment and are therefore costly. NIRS is a new methodology for brain research and brain function testing, and has applications in various areas of medicine, being used not only in research, but also in clinical medicine.[23–25,48] NIRS has been approved for identifying the language-dominant hemisphere before brain surgery and measuring epileptic foci.[49] In human studies comparing NIRS and fMRI,[50–52] a correlation was seen between blood-oxygen-level-dependent signal and oxy-Hb concentration as measured by NIRS. In brain function analysis, the detection sensitivity of NIRS is comparable to that of fMRI, but the time resolution of NIRS is greater. Furthermore, the advantages of NIRS are convenience, bedside analysis, non-invasiveness, free task setting and low cost.

Here, we used multichannel NIRS to measure the changes in oxy-Hb concentration during task performance from the frontal to temporal regions of the cortex in MHE patients and compared the results with those of liver cirrhosis without MHE. In all subjects, oxy-Hb increased during task performance and gradually decreased after the completion of task performance. However, the time-dependent changes in the degree of increase in oxy-Hb concentration differed between patients with and without MHE. The degree of increase in oxy-Hb concentration during task performance was smaller and more gradual in MHE compared to non-MHE patients. The increase of the oxy-Hb concentration reflects the increase of cerebral blood volume in the area of the brain activated by the task. Iversen *et al.* found that the cerebral oxygen consumption and blood flow were both reduced in cirrhotic patients with an acute episode of OHE[16]and that the oxygen delivery was approximately twice the oxygen consumption, indicating that oxygen delivery or blood flow was not a limiting factor for the oxygen consumption. Consequently, cerebral blood flow seems to be reduced as a result of diminished cerebral oxygen requirement during HE, and not vice versa.[16] It is reported that neuron-to-astrocyte signaling is a key mechanism in functional hyperemia,[17–19,53,54] and that function of astrocytes is impaired in hepatic encephalopathy patients.[20–22] Therefore, impaired astrocyte-mediated control of cerebral microcirculation can result in slow increase of cerebral blood flow during task performance in MHE patients. Thus, the sluggish increase in cerebral blood flow seen in MHE in the present study may reflect the impaired brain activity and dysfunction of astrocytes and impaired cerebral oxygen metabolism in these patients.

There are several limitations in the present study. The number of patients was not enough to make a comparison stratified by Child grade. We would like to analyze this important point in a future study. It may be possible that cerebral oxy-Hb may change due to aging or by the arteriosclerotic changes. In the present study, age was not related to NIRS results. All patients were examined by brain MRI or brain CT and they had no apparent brain structural disease including brain infarction. However, it was not possible to evaluate the arteriosclerotic changes. This may be another limitation of this study. Many neuropsychological function tests, such as number connection test, light/sound reaction time, inhibitory control test, WAIS or electro-psychological tests including EEG, cerebral evoked potential, p300 event-related potential, PHES and critical flicker test have been employed for the diagnosis of MHE. In Japan, Kato and colleagues established the computer-aided quantitative neuropsychological function test system called NP-test.[7] However, these tests were not simultaneously measured in the present study. Because we recognize the importance of comparing NIRS with other tests, we would like to solve this issue in future study.

In conclusion, NIRS, with its high degree of time resolution, enabled us to identify the characteristic time course of oxy-Hb concentration changes during tasks in MHE. The observations imply that cerebral oxygen supply and metabolism is poorly reactive in MHE, which may be related to the pathogenesis of latent impairment of brain activity.

REFERENCES

1 Bajaj JS, Hafeezullah M, Hoffmann RG *et al.* Navigation skill impairment: another dimension of the driving difficulties in minimal hepatic encephalopathy. *Hepatology* 2008; 47: 596–604.
2 Bajaj JS, Pinkerton SD, Sanyal AJ, Heuman DM. Diagnosis and treatment of minimal hepatic encephalopathy to prevent motor vehicle accidents: a cost-effectiveness analysis. *Hepatology* 2012; 55: 1164–71.

3 Dhiman RK, Kurmi R, Thumburu KK *et al.* Diagnosis and prognostic significance of minimal hepatic encephalopathy in patients with cirrhosis of liver. *Dig Dis Sci* 2010; **55**: 2381–90.
4 Bajaj JS, Heuman DM, Wade JB *et al.* Rifaximin improves driving simulator performance in a randomized trial of patients with minimal hepatic encephalopathy. *Gastroenterology* 2011; **140**: 478–87 e1.
5 Prasad S, Dhiman RK, Duseja A, Chawla YK, Sharma A, Agarwal R. Lactulose improves cognitive functions and health-related quality of life in patients with cirrhosis who have minimal hepatic encephalopathy. *Hepatology* 2007; **45**: 549–59.
6 Sharma P, Sharma BC, Agrawal A, Sarin SK. Primary prophylaxis of overt hepatic encephalopathy in patients with cirrhosis: an open labeled randomized controlled trial of lactulose versus no lactulose. *J Gastroenterol Hepatol* 2012; **27**: 1329–35.
7 Kato A, Watanabe Y, Sawara K, Suzuki K. Diagnosis of sub-clinical hepatic encephalopathy by Neuropsychological Tests (NP-tests). *Hepatol Res* 2008; **38** (Suppl 1): S122–7.
8 Kircheis G, Wettstein M, Timmermann L, Schnitzler A, Haussinger D. Critical flicker frequency for quantification of low-grade hepatic encephalopathy. *Hepatology* 2002; **35**: 357–66.
9 Romero-Gomez M, Cordoba J, Jover R *et al.* Value of the critical flicker frequency in patients with minimal hepatic encephalopathy. *Hepatology* 2007; **45**: 879–85.
10 Amodio P, Campagna F, Olianas S *et al.* Detection of minimal hepatic encephalopathy: normalization and optimization of the Psychometric Hepatic Encephalopathy Score. A neuropsychological and quantified EEG study. *J Hepatol* 2008; **49**: 346–53.
11 Davies MG, Rowan MJ, MacMathuna P, Keeling PW, Weir DG, Feely J. The auditory P300 event-related potential: an objective marker of the encephalopathy of chronic liver disease. *Hepatology* 1990; **12**: 688–94.
12 Kugler CF, Lotterer E, Petter J *et al.* Visual event-related P300 potentials in early portosystemic encephalopathy. *Gastroenterology* 1992; **103**: 302–10.
13 Bajaj JS, Hafeezullah M, Franco J *et al.* Inhibitory control test for the diagnosis of minimal hepatic encephalopathy. *Gastroenterology* 2008; **135**: 1591–600 e1.
14 Sharma P, Kumar A, Singh S, Tyagi P. Inhibitory control test, critical flicker frequency, and psychometric tests in the diagnosis of minimal hepatic encephalopathy in cirrhosis. *Saudi J Gastroenterol* 2013; **19**: 40–4.
15 Goldbecker A, Weissenborn K, Hamidi Shahrezaei G *et al.* Comparison of the most favoured methods for the diagnosis of hepatic encephalopathy in liver transplantation candidates. *Gut* 2013. doi: 10.1136/gutjnl-2012-303262.
16 Iversen P, Sorensen M, Bak LK *et al.* Low cerebral oxygen consumption and blood flow in patients with cirrhosis and an acute episode of hepatic encephalopathy. *Gastroenterology* 2009; **136**: 863–71.
17 Gordon GR, Choi HB, Rungta RL, Ellis-Davies GC, MacVicar BA. Brain metabolism dictates the polarity of astrocyte control over arterioles. *Nature* 2008; **456**: 745–9.
18 Takano T, Tian GF, Peng W *et al.* Astrocyte-mediated control of cerebral blood flow. *Nat Neurosci* 2006; **9**: 260–7.
19 Magistretti PJ. Neuron-glia metabolic coupling and plasticity. *J Exp Biol* 2006; **209**: 2304–11.
20 Gorg B, Qvartskhava N, Keitel V *et al.* Ammonia induces RNA oxidation in cultured astrocytes and brain in vivo. *Hepatology* 2008; **48**: 567–79.
21 Albrecht J, Norenberg MD. Glutamine: a Trojan horse in ammonia neurotoxicity. *Hepatology* 2006; **44**: 788–94.
22 Lemberg A, Fernandez MA. Hepatic encephalopathy, ammonia, glutamate, glutamine and oxidative stress. *Ann Hepatol* 2009; **8**: 95–102.
23 Maki A, Yamashita Y, Ito Y, Watanabe E, Mayanagi Y, Koizumi H. Spatial and temporal analysis of human motor activity using noninvasive NIR topography. *Med Phys* 1995; **22**: 1997–2005.
24 Kameyama M, Fukuda M, Yamagishi Y *et al.* Frontal lobe function in bipolar disorder: a multichannel near-infrared spectroscopy study. *Neuroimage* 2006; **29**: 172–84.
25 Suto T, Fukuda M, Ito M, Uehara T, Mikuni M. Multichannel near-infrared spectroscopy in depression and schizophrenia: cognitive brain activation study. *Biol Psychiatry* 2004; **55**: 501–11.
26 Takizawa R, Kasai K, Kawakubo Y *et al.* Reduced frontopolar activation during verbal fluency task in schizophrenia: a multi-channel near-infrared spectroscopy study. *Schizophr Res* 2008; **99**: 250–62.
27 Groeneweg M, Quero JC, De Bruijn I *et al.* Subclinical hepatic encephalopathy impairs daily functioning. *Hepatology* 1998; **28**: 45–9.
28 Marchesini G, Bianchi G, Amodio P *et al.* Factors associated with poor health-related quality of life of patients with cirrhosis. *Gastroenterology* 2001; **120**: 170–8.
29 Schomerus H, Hamster W, Blunck H, Reinhard U, Mayer K, Dolle W. Latent portasystemic encephalopathy. I. Nature of cerebral functional defects and their effect on fitness to drive. *Dig Dis Sci* 1981; **26**: 622–30.
30 Wein C, Koch H, Popp B, Oehler G, Schauder P. Minimal hepatic encephalopathy impairs fitness to drive. *Hepatology* 2004; **39**: 739–45.
31 Ferenci P, Lockwood A, Mullen K, Tarter R, Weissenborn K, Blei AT. Hepatic encephalopathy – definition, nomenclature, diagnosis, and quantification: final report of the working party at the 11th World Congresses of Gastroenterology, Vienna, 1998. *Hepatology* 2002; **35**: 716–21.
32 Ortiz M, Jacas C, Cordoba J. Minimal hepatic encephalopathy: diagnosis, clinical significance and recommendations. *J Hepatol* 2005; **42** (Suppl): S45–53.
33 Niedermeyer E. The clinical relevance of EEG interpretation. *Clin Electroencephalogr* 2003; **34**: 93–8.

34 Amodio P, Pellegrini A, Ubiali E *et al.* The EEG assessment of low-grade hepatic encephalopathy: comparison of an artificial neural network-expert system (ANNES) based evaluation with visual EEG readings and EEG spectral analysis. *Clin Neurophysiol* 2006; **117:** 2243–51.
35 Amodio P, Marchetti P, Del Piccolo F *et al.* Spectral versus visual EEG analysis in mild hepatic encephalopathy. *Clin Neurophysiol* 1999; **110:** 1334–44.
36 Sagales T, Gimeno V, de la Calzada MD, Casellas F, Dolors Macia M, Villar Soriano M. Brain mapping analysis in patients with hepatic encephalopathy. *Brain Topogr* 1990; **2:** 221–8.
37 Bajaj JS, Cordoba J, Mullen KD *et al.* Review article: the design of clinical trials in hepatic encephalopathy – an International Society for Hepatic Encephalopathy and Nitrogen Metabolism (ISHEN) consensus statement. *Aliment Pharmacol Ther* 2011; **33:** 739–47.
38 Ross BD, Danielsen ER, Bluml S. Proton magnetic resonance spectroscopy: the new gold standard for diagnosis of clinical and subclinical hepatic encephalopathy? *Dig Dis* 1996; **14** (Suppl 1): 30–9.
39 Ross BD, Jacobson S, Villamil F *et al.* Subclinical hepatic encephalopathy: proton MR spectroscopic abnormalities. *Radiology* 1994; **193:** 457–63.
40 Minguez B, Garcia-Pagan JC, Bosch J *et al.* Noncirrhotic portal vein thrombosis exhibits neuropsychological and MR changes consistent with minimal hepatic encephalopathy. *Hepatology* 2006; **43:** 707–14.
41 Kato A, Suzuki K, Kaneta H, Obara H, Fujishima Y, Sato S. Regional differences in cerebral glucose metabolism in cirrhotic patients with subclinical hepatic encephalopathy using positron emission tomography. *Hepatol Res* 2000; **17:** 237–45.
42 Taylor-Robinson SD, Sargentoni J, Mallalieu RJ *et al.* Cerebral phosphorus-31 magnetic resonance spectroscopy in patients with chronic hepatic encephalopathy. *Hepatology* 1994; **20:** 1173–8.
43 Laubenberger J, Haussinger D, Bayer S, Gufler H, Hennig J, Langer M. Proton magnetic resonance spectroscopy of the brain in symptomatic and asymptomatic patients with liver cirrhosis. *Gastroenterology* 1997; **112:** 1610–6.
44 Kale RA, Gupta RK, Saraswat VA *et al.* Demonstration of interstitial cerebral edema with diffusion tensor MR imaging in type C hepatic encephalopathy. *Hepatology* 2006; **43:** 698–706.
45 Lockwood AH, Yap EW, Rhoades HM, Wong WH. Altered cerebral blood flow and glucose metabolism in patients with liver disease and minimal encephalopathy. *J Cereb Blood Flow Metab* 1991; **11:** 331–6.
46 Lockwood AH. Positron emission tomography in the study of hepatic encephalopathy. *Metab Brain Dis* 2002; **17:** 431–5.
47 Ahl B, Weissenborn K, van den Hoff J *et al.* Regional differences in cerebral blood flow and cerebral ammonia metabolism in patients with cirrhosis. *Hepatology* 2004; **40:** 73–9.
48 Cyranoski D. Neuroscience: thought experiment. *Nature* 2011; **469:** 148–9.
49 Watanabe E, Nagahori Y, Mayanagi Y. Focus diagnosis of epilepsy using near-infrared spectroscopy. *Epilepsia* 2002; **43** (Suppl 9): 50–5.
50 Strangman G, Culver JP, Thompson JH, Boas DA. A quantitative comparison of simultaneous BOLD fMRI and NIRS recordings during functional brain activation. *Neuroimage* 2002; **17:** 719–31.
51 Sassaroli A, deB Frederick B, Tong Y, Renshaw PF, Fantini S. Spatially weighted BOLD signal for comparison of functional magnetic resonance imaging and near-infrared imaging of the brain. *Neuroimage* 2006; **33:** 505–14.
52 Huppert TJ, Hoge RD, Diamond SG, Franceschini MA, Boas DA. A temporal comparison of BOLD, ASL, and NIRS hemodynamic responses to motor stimuli in adult humans. *Neuroimage* 2006; **29:** 368–82.
53 Zonta M, Angulo MC, Gobbo S *et al.* Neuron-to-astrocyte signaling is central to the dynamic control of brain microcirculation. *Nat Neurosci* 2003; **6:** 43–50.
54 Schummers J, Yu H, Sur M. Tuned responses of astrocytes and their influence on hemodynamic signals in the visual cortex. *Science* 2008; **320:** 1638–43.

Hepatology Research

Hepatology Research 2013 doi: 10.1111/hepr.12179

Original Article

Prospective comparison of real-time tissue elastography and serum fibrosis markers for the estimation of liver fibrosis in chronic hepatitis C patients

Nobuharu Tamaki,[1] Masayuki Kurosaki,[1] Shuya Matsuda,[1] Toru Nakata,[1] Masaru Muraoka,[1] Yuichiro Suzuki,[1] Yutaka Yasui,[1] Shoko Suzuki,[1] Takanori Hosokawa,[1] Takashi Nishimura,[1] Ken Ueda,[1] Kaoru Tsuchiya,[1] Hiroyuki Nakanishi,[1] Jun Itakura,[1] Yuka Takahashi,[1] Kotaro Matsunaga,[2,4] Kazuhiro Taki,[2] Yasuhiro Asahina[3] and Namiki Izumi[1]

Divisions of [1]Gastroenterology and Hepatology and [2]Pathology, Musashino Red Cross Hospital, [3]Division of Gastroenterology and Hepatology, Tokyo Medical and Dental University, Tokyo and [4]Division of Gastroenterology and Hepatology, St Marianna University School of Medicine, Kanagawa, Japan

Aim: Real-time tissue elastography (RTE) is a non-invasive method for the measurement of tissue elasticity using ultrasonography. Liver fibrosis (LF) index is a quantitative method for evaluation of liver fibrosis calculated by RTE image features. This study aimed to investigate the significance of LF index for predicting liver fibrosis in chronic hepatitis C patients.

Methods: In this prospective study, 115 patients with chronic hepatitis C who underwent liver biopsy were included, and the diagnostic accuracy of LF index and serum fibrosis markers was evaluated.

Results: RTE imaging was successfully performed on all patients. Median LF index in patients with F0–1, F2, F3 and F4 were 2.61, 3.07, 3.54 and 4.25, respectively, demonstrating a stepwise increase with liver fibrosis progression ($P < 0.001$). LF index (odds ratio [OR] = 5.3, 95% confidence interval [CI] = 2.2–13.0) and platelet count (OR = 0.78, 95% CI = 0.68–0.89) were independently associated with the presence of advanced fibrosis (F3–4). Further, LF index was independently associated with the presence of minimal fibrosis (F0–1) (OR = 0.25, 95% CI = 0.11–0.55). The area under the receiver–operator curve (AUROC) of LF index for predicting advanced fibrosis (0.84) was superior to platelets (0.82), FIB-4 index (0.80) and aspartate aminotransferase/platelet ratio index (APRI) (0.76). AUROC of LF index (0.81) was superior to platelets (0.73), FIB-4 index (0.79) and APRI (0.78) in predicting minimal fibrosis.

Conclusion: LF index calculated by RTE is useful for predicting liver fibrosis, and diagnostic accuracy of LF index is superior to serum fibrosis markers.

Key words: chronic hepatitis C, fibrosis, liver fibrosis index, real-time tissue elastography

INTRODUCTION

AN ADVANCED STAGE of liver fibrosis in chronic hepatitis C (CHC) is associated with hepatocellular carcinoma development and complications such as esophageal variceal bleeding and liver failure.[1,2] Therefore, accurate evaluation of the stage of liver fibrosis is most important in clinical practice. Liver biopsy is considered to be the golden standard for diagnosis of liver fibrosis.[3–5] However, this method may be inaccurate because of sampling errors and interobserver variations.[6,7]

Improvements in a variety of non-invasive methods for evaluating liver fibrosis have recently emerged as alternatives to liver biopsy. Liver fibrosis was reportedly predicted by measurement of liver stiffness using transient elastography[8,9] and acoustic radiation force impulse (ARFI).[10,11] As assessed by blood laboratory tests, the aspartate aminotransferase (AST)/alanine

Correspondence: Dr Namiki Izumi, Department of Gastroenterology and Hepatology, Musashino Red Cross Hospital, 1-26-1 Kyonan-cho, Musashino-shi, Tokyo 180-8610, Japan. Email: nizumi@musashino.jrc.or.jp

Conflict of interest: The authors who have taken part in this study declare that they do not have anything to disclose regarding funding or conflict of interest with respect to this manuscript.

Received 28 January 2013; revision 20 May 2013; accepted 29 May 2013.

aminotransferase (ALT) ratio,[12] AST/platelet ratio index (APRI),[13,14] and FIB-4 index[15,16] have been reported to be useful for the prediction of liver fibrosis. We previously reported that the FIB-4 index is useful for the prediction of liver fibrosis progression.[17]

Real-time tissue elastography (RTE) is a non-invasive method for the measurement of tissue elasticity using ultrasonography.[18] RTE calculates the relative hardness of tissue from the degree of tissue distortion and displays this information as a color image. RTE was recently reported to be useful for predicting liver fibrosis.[19,20] To increase the objectivity of the evaluation, an image analysis method to evaluate the strain image features and a new algorithm to deliver an index were proposed. Liver fibrosis (LF) index is a quantitative method for evaluation of liver fibrosis that is calculated by nine RTE image features, and the significance of LF index for predicting liver fibrosis has been reported.[21,22]

In the present study, we prospectively investigated the significance of LF index calculated by RTE for the prediction of liver fibrosis in CHC patients. Further, diagnostic accuracy for liver fibrosis was compared between LF index and serum fibrosis markers.

METHODS

Patients

A TOTAL OF 127 consecutive patients with CHC were prospectively investigated. All patients underwent liver biopsy at Musashino Red Cross Hospital between February 2011 and November 2012. Exclusion criteria comprised the following: (i) co-infection with hepatitis B virus ($n = 1$); (ii) co-infection with HIV ($n = 1$); (iii) history of autoimmune hepatitis or primary biliary cirrhosis ($n = 3$); (iv) alcohol abuse (intake of alcohol equivalent to pure alcohol ≥40 g/day) ($n = 0$); (v) portal tracts of biopsy sample of less than five ($n = 7$); and (vi) presence of serious heart disease ($n = 0$). After exclusion, 115 patients were enrolled in this study. Written informed consent was obtained from each patient and the study protocol conformed to the ethical guidelines of the Declaration of Helsinki and was approved by the institutional ethics review committees (application no. 24007).

Histological evaluation

Liver biopsy specimens were laparoscopically obtained using 13-G needles ($n = 93$). When laparoscopy was not conducted due to a history of upper abdominal surgery, percutaneous ultrasound-guided liver biopsy was performed using 15-G needles ($n = 22$). Specimens were fixed, paraffin-embedded, and stained with hematoxylin–eosin and Masson-trichrome. A biopsy sample with minimum portal tracts of five was required for diagnosis. All liver biopsy samples were independently evaluated by two senior pathologists who were blinded to the clinical data. Fibrosis staging was categorized according to the METAVIR score:[23] F0, no fibrosis; F1, portal fibrosis without septa; F2, portal fibrosis with few septa; F3, numerous septa without cirrhosis; and F4, cirrhosis. Activity of necroinflammation was graded on a scale of 0–3: A0, no activity; A1, mild activity; A2, moderate activity; and A3, severe activity. Percentage of steatosis was quantified by determining the average proportion of hepatocytes affected by steatosis and graded on a scale of 0–3: grade 0, no steatosis; grade 1, 1–33%; grade 2, 34–66%; and grade 3, 67% and over.

Clinical and biological data

The age and sex of the patients were recorded. Serum samples were collected within 1 day prior to liver biopsy and the following variables were obtained through serum sample analysis: AST, ALT and platelet count. FIB-4 index and APRI were calculated according to the published formula appropriate to each measure.[13,15]

RTE and LF index

Real-time tissue elastography was performed using HI VISION Preirus (Hitachi Aloka Medical, Tokyo, Japan) and the EUP-L52 linear probe (3–7 MHz; Hitachi Aloka Medical) within 3 days of liver biopsy. RTE was performed on the right lobe of the liver through the intercostal space. An RTE image was induced by heartbeats. Five RTE images were collected for each patient and analyzed to calculate nine image features. RTE method and the equation that calculates LF index using nine image features has been previously detailed.[22] Results are expressed as mean LF index of all measurements. Two hepatologists (N. T. and K. Tsuchiya, with 8 and 16 years of experience, respectively) performed RTE. In 32 patients with CHC, LF index was measured independently by two examiners. The correlation coefficient of LF index between two examiners was 0.85 ($P \leq 0.001$).

Statistical analysis

Correlations between LF index and histological fibrosis stage were analyzed using Spearman's rank correlation coefficients. Categorical variables were compared using Fisher's exact test, and continuous variables were compared using Mann–Whitney *U*-test. $P < 0.05$ was considered statistically significant. Logistic regression was

used for multivariate analysis. Receiver-operator curves (ROC) were constructed, and the area under the ROC (AUROC) was calculated. Optimal cut-off values were selected, to maximize sensitivity, specificity and diagnostic accuracy. Sensitivity, specificity, positive predictive value (PPV) and negative predictive value (NPV) were calculated by using cut-offs obtained by ROC. SPSS software ver. 15.0 (SPSS, Chicago, IL, USA) was used for analyses.

RESULTS

Patient characteristics

THE CHARACTERISTICS OF all 115 patients are listed in Table 1. F0–1 was diagnosed in 52 cases (45%), F2 in 31 (27%), F3 in 20 (17%) and F4 in 12 (11%). Mean values of LF index of F0 (2.62) and F1 (2.60) were not significantly different ($P = 0.9$), and only six patients with F0 were included in this study. Therefore, patients with F0 and F1 were integrated for the analysis. RTE imaging was successfully performed in all patients, and LF index was calculated.

Relationship between histological findings and LF index by RTE

The median value of LF index compared with the METAVIR fibrosis stage is shown in Figure 1. Median LF index in patients with F0–1, F2, F3 and F4 were 2.61, 3.07, 3.54 and 4.25, respectively, demonstrating a stepwise increase with liver fibrosis progression ($P < 0.001$). LF index of each fibrosis stage significantly differed from each other (F0–1 vs F2, $P < 0.001$; F0–1 vs F3, $P < 0.001$; F0–1 vs F4, $P < 0.001$; F2 vs F3, $P = 0.009$; F2 vs F4, $P = 0.001$). On the other hand, mean values of LF index in patients with steatosis grade 0, 1 and 2 were 2.99, 3.29 and 2.60, respectively, demonstrating no significant correlation (Fig. 2a). LF index was compared with steatosis grade for each fibrosis stage. LF index was not significantly different between patients with steatosis and without steatosis (Fig. 2b).

Liver fibrosis index was compared with histological activity. A significant correlation existed between histological activity and fibrosis stage. Therefore, the relationship between LF index and histological activity was examined by each fibrosis stage. In patients with F0–1, the mean LF index of A1, A2 and A3 was 2.60, 2.58 and 2.40, respectively, demonstrating no significant correlation. Similarly, in patients with F2, F3 and F4, there was no significant correlation between LF index and histological activity (Fig. 3).

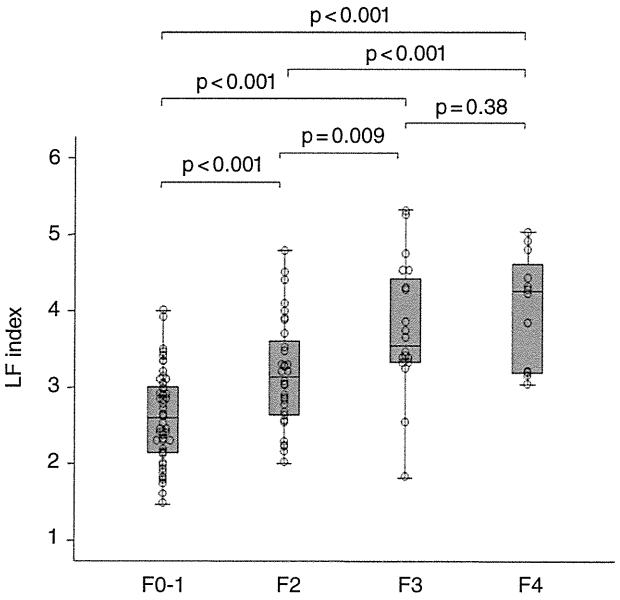

Figure 1 Correlation between liver fibrosis (LF) index calculated by real-time tissue elastography and fibrosis stage. Box plot of the LF index is shown according to each fibrosis stage. The bottom and top of each box represent the 25th and 75th percentiles, giving the interquartile range. The line through the box indicates the median value, and error bar indicates minimum and maximum non-extreme values.

Table 1 Patient characteristics

Characteristics	Patients ($n = 115$)
Female/male	68/47
Age (years)	57.9 ± 10.9
AST (IU/L)	55.7 ± 44.9
ALT (IU/L)	63.2 ± 56.3
Platelet counts ($\times 10^9$/L)	162 ± 53
Portal tracts of biopsy samples	12.6 ± 5.0
Fibrosis stage	
F0–1 (%)	51 (44)
F2 (%)	32 (28)
F3 (%)	20 (17)
F4 (%)	12 (11)
Histological activity	
A0 (%)	0 (0)
A1 (%)	75 (65)
A2 (%)	34 (30)
A3 (%)	6 (5)
Steatosis grade	
Grade 0 (%)	65 (57)
Grade 1 (%)	47 (41)
Grade 2 (%)	3 (2)
Grade 3 (%)	0 (0)

ALT, alanine aminotransferase; AST, aspartate aminotransferase.

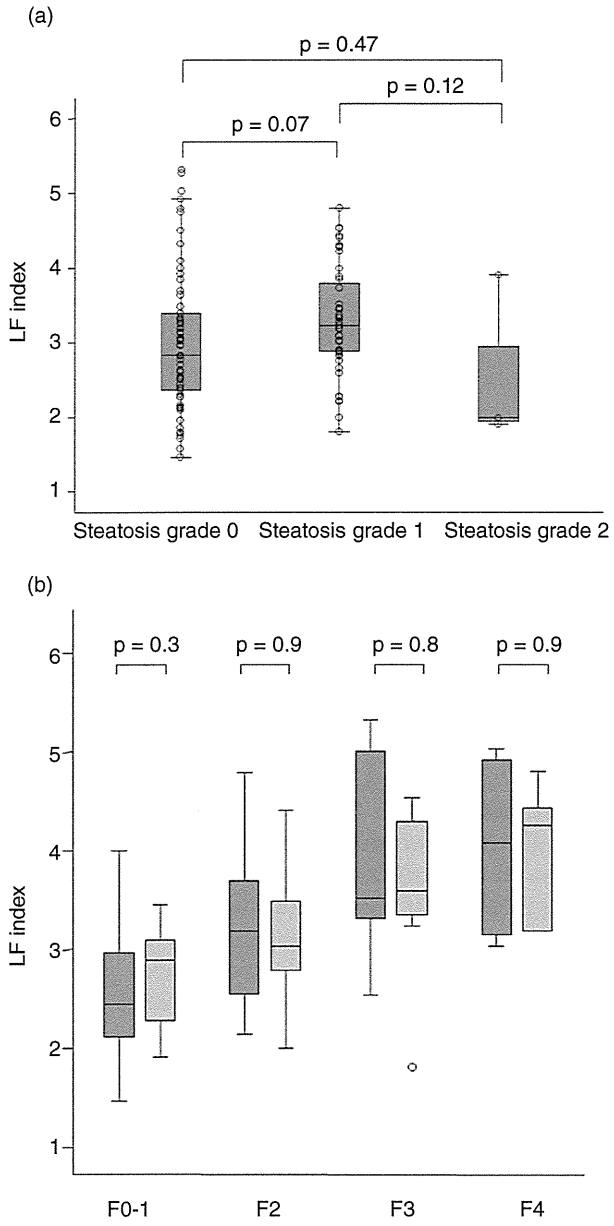

Figure 2 (a) Correlation between liver fibrosis (LF) index and steatosis grade. Box plot of the LF index is shown according to each steatosis grade. The bottom and top of each box represent the 25th and 75th percentiles, giving the interquartile range. The line through the box indicates the median value, and error bar indicates minimum and maximum non-extreme values. (b) Box plot of LF index for each fibrosis stage in relation to degree of steatosis grade. The bottom and top of each box represent the 25th and 75th percentiles, giving the interquartile range. The line through the box indicates the median value, and error bar indicates minimum and maximum non-extreme values. Dark grey bar chart indicates steatosis grade 0. Light grey bar chart indicates steatosis grade 1–2.

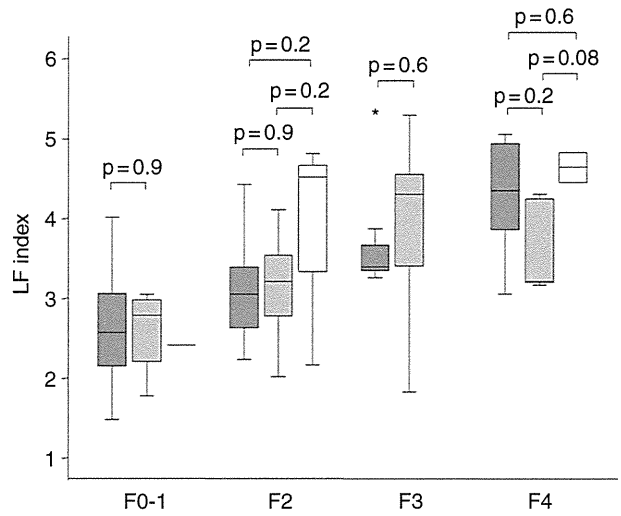

Figure 3 Box plot of liver fibrosis (LF) index for each fibrosis stage in relation to degree of necroinflammatory activity. The bottom and top of each box represent the 25th and 75th percentiles, giving the interquartile range. The line through the box indicates the median value, and error bar indicates minimum and maximum non-extreme values. Dark grey bar chart indicates activity grade 1. Light grey bar chart indicates activity grade 2. White bar chart indicates activity grade 3.

Comparison of variables associated with the presence of advanced fibrosis (F3–4) by univariate and multivariate analysis

Variables associated with the presence of advanced fibrosis (F3–4) were assessed by univariate and multivariate analysis (Table 2). The variables of age ($P = 0.03$) and LF index ($P < 0.001$) were significantly higher, and the variable of platelets ($P < 0.001$) was significantly lower in patients with advanced fibrosis than in patients with F0–2. Multivariate analysis showed that LF index (odds ratio [OR] = 5.3, 95% confidence interval [CI] =2.2–13.0) and platelets (OR = 0.78, 95% CI = 0.68–0.89) were independently associated with the presence of advanced fibrosis.

Comparison of variables associated with the presence of minimal fibrosis (F0–1) by univariate and multivariate analysis

Variables associated with the presence of minimal fibrosis (F0–1) were assessed by univariate and multivariate analysis (Table 3). The variables of age ($P < 0.001$), AST ($P = 0.02$) and LF index ($P < 0.001$) were significantly lower, and the variable of platelets ($P < 0.001$) was significantly higher in F0–1 patients than F2–4 patients.

Table 2 Variables associated with the presence of advanced fibrosis (F3–4) by univariate and multivariate analysis

	F0–2 ($n = 83$)	F3–4 ($n = 32$)	*P*-value (Univariate)	Odds ratio (95% CI) (Multivariate)
Age (years)	56.6 ± 10.9	61.3 ± 10.4	0.03	
Sex (female/male)	51/32	17/15	0.41	
AST (IU/L)	52.3 ± 43.3	64.4 ± 48.3	0.19	
ALT (IU/L)	62.9 ± 60.6	63.9 ± 44.2	0.93	
Platelets ($\times 10^9$/L)	179 ± 47	117 ± 42	<0.001	0.78 (0.68–0.89)
LF index	2.81 ± 0.69	3.86 ± 0.81	<0.001	5.30 (2.16–13.0)

ALT, alanine aminotransferase; AST, aspartate aminotransferase; CI, confidence interval; LF, liver fibrosis.

Multivariate analysis showed that LF index was independently associated with the presence of minimal fibrosis (OR = 0.25, 95% CI = 0.11–0.55).

Diagnostic accuracy of RTE and serum fibrosis markers

Receiver-operator curves of LF index, platelets, FIB-4 index and APRI for predicting advanced fibrosis (F3–4), and minimal fibrosis (F0–1) were plotted, as shown in Figure 4. AUROC of LF index for predicting advanced fibrosis (0.84) was superior to platelets (0.82), FIB-4 index (0.80) and APRI (0.76). Similarly, for predicting minimal fibrosis, AUROC of LF index (0.81) was superior to platelets (0.73), FIB-4 index (0.79) and APRI (0.78). The corresponding sensitivities, specificities, PPV and NPV are detailed in Table 4.

DISCUSSION

IMPROVEMENTS IN VARIOUS methods for prediction of liver fibrosis have recently emerged as alternatives to liver biopsy. RTE is a non-invasive method for the measurement of tissue elasticity using ultrasonography. The utility of RTE for evaluating liver fibrosis is reported in a few studies.[18–22] However, for utilizing LF index, one of the equations used to calculate tissue elasticity by RTE is still unclear. The aim of this study was to investigate the significance of LF index for the prediction of liver fibrosis in CHC patients.

In this prospective study, we found that LF index is a useful predictive factor for diagnosis of the fibrosis stage in CHC patients. Increase in LF index significantly correlated with progression of the fibrosis stage and LF index was able to predict the presence of advanced fibrosis and minimal fibrosis. Previous studies reported the utility of LF index for prediction of the liver fibrosis stage.[21,22] In this study, LF index differed significantly between patients with F0–1 and F2; thus, LF index was especially useful for prediction of minimal fibrosis. This may be due to a sufficient number of patients with F0–1 and F2 included in the present study. This is an advantage of LF index because other quantitative methods by RTE could not discriminate patients with F0–1 and F2.[19,20] On the other hand, there is a possibility that a similar result may be obtained for differentiation of F3 and F4 if a large number of patients with advanced fibrosis was included.

Previous studies did not compare the diagnostic accuracy of LF index and serum fibrosis markers. We revealed that LF index performed better than serum fibrosis

Table 3 Variables associated with the presence of minimal fibrosis (F0–1) by univariate and multivariate analysis

	F0–1 ($n = 51$)	F2–4 ($n = 64$)	*P*-value (Univariate)	Odds ratio (95% CI) (Multivariate)
Age (years)	54.0 ± 11.9	61.0 ± 9.0	<0.001	
Sex (female/male)	31/20	37/27	0.74	
AST (IU/L)	44.5 ± 42.6	64.6 ± 44.9	0.02	
ALT (IU/L)	53.0 ± 56.3	71.3 ± 55.5	0.08	
Platelets ($\times 10^9$/L)	186 ± 47	142 ± 50	<0.001	
LF index	2.60 ± 0.59	3.51 ± 0.84	<0.001	0.25 (0.11–0.55)

ALT, alanine aminotransferase; AST, aspartate aminotransferase; CI, confidence interval; LF, liver fibrosis.

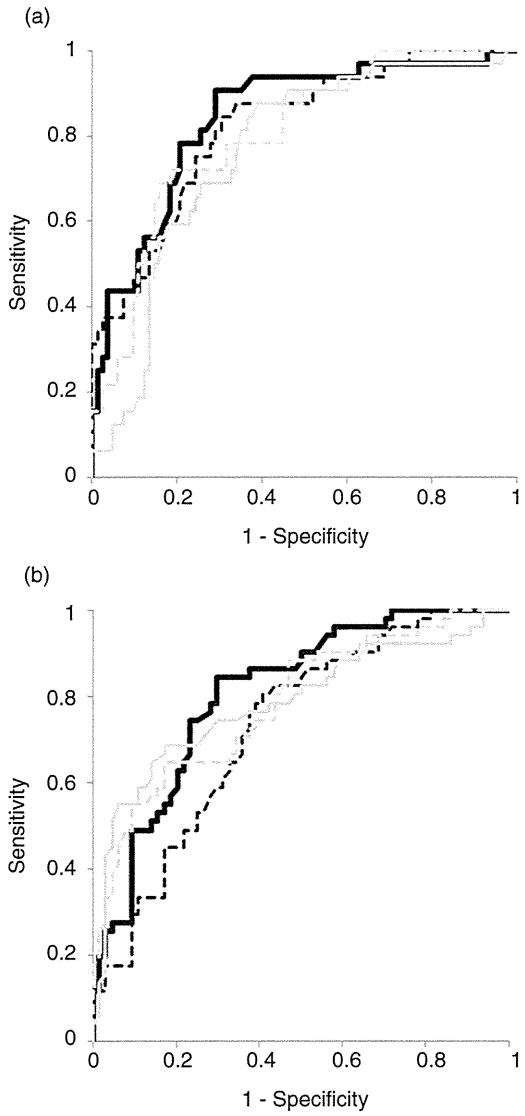

Figure 4 Receiver–operator curves (ROC) of liver fibrosis (LF) index and serum fibrosis markers. (a) ROC for diagnosis of significant fibrosis (F3–4). (b) ROC for diagnosis of minimal fibrosis (F0–1). —, LF index; ·---·, platelets; ——, aspartate aminotransferase-to-platelet ratio index; - - -, FIB-4 index.

markers based on blood laboratory tests for predicting liver fibrosis.

Transient elastography has been most commonly used to measure liver stiffness and is established in clinical practice to evaluate liver fibrosis.[8,9] RTE exhibits some advantages compared with transient elastography. In this study, RTE imaging was successfully performed in all patients, and LF index was calculated. Although transient elastography has high diagnostic capabilities when it comes to liver fibrosis, measurements are sometimes impossible in patients with severe obesity and ascites.[24] Reproducibility of transient elastography was reportedly lower in patients with steatosis, inflammation, increased body mass index and lower degrees of liver fibrosis.[25–27] On the other hand, LF index is measured by ultrasound guidance that facilitates the identification of a suitable location for elastographic measurement, thereby resulting in a higher number of patients with valid results.

Unlike transient elastography, another advantage of LF index is that the results are not influenced by the presence of inflammation and steatosis. It was reported that LF index is not useful in patients with steatosis.[22] However, LF index was not significantly different between patients with and without steatosis in the present study even after stratification by fibrosis stage. Thus, LF index was useful for prediction of fibrosis in CHC patients regardless of steatosis. Because LF index of each activity grade and steatosis grade did not differ from each other, estimation of liver fibrosis by LF index demonstrated higher reproducibility than transient elastography.

In previously reports, diagnostic accuracy of liver fibrosis using RTE was inferior to transient elastography;[28] however, other studies have reported contrasting results.[19] The reason for this variability is probably because RTE technology and the equations used to calculate tissue elasticity are rapidly changing. The utility of elastic ratio, another RTE method for evaluation of liver fibrosis, was reported.[20] The elastic ratio is the ratio between the tissue compressibility of the liver and that of the intrahepatic small vessel. The AUROC of elastic ratio for predicting advanced fibrosis was 0.94 and was superior to LF index. Further, ARFI and real-time shear wave elastography were reported to have a high diagnostic accuracy of liver fibrosis.[10,11,29] There are currently no studies that directly compare LF index and those methods for diagnostic value of liver fibrosis. Therefore, further studies are needed to fully explore the potential of RTE, especially with regard to LF index.

Our study had several limitations. The number of patients with advanced fibrosis was small. The potential of LF index to differentiate patients with F3 and F4 needs to be explored with a large number of patients. Further, validation study is needed to evaluate the diagnostic accuracy of fibrosis stage, especially in comparison with other modalities.

In conclusion, LF index calculated by RTE is useful for predicting liver fibrosis, and diagnostic accuracy of LF index is superior to that of serum fibrosis markers.

Table 4 Diagnostic performance of LF index and serum fibrosis markers

	F0–2 vs F3–4					F0–1 vs F2–4				
	AUROC	Sensitivity (%)	Specificity (%)	PPV (%)	NPV (%)	AUROC	Sensitivity (%)	Specificity (%)	PPV (%)	NPV (%)
LF index	0.84	90.6	71.1	54.7	95.2	0.81	84.3	70.3	69.4	84.9
Platelets	0.82	87.5	66.3	50.0	93.2	0.73	80.4	59.4	61.2	79.2
FIB-4 index	0.80	71.9	81.9	60.5	88.3	0.79	54.9	90.6	82.3	71.6
APRI	0.76	87.5	61.4	46.7	92.7	0.78	64.7	85.9	78.6	75.3

APRI, aspartate aminotransferase/platelet ratio index; AUROC, area under the receiver–operator curve; NPV, negative predictive value; PPV, positive predictive value.

ACKNOWLEDGMENT

THIS STUDY WAS supported by a Grant-in-Aid from Ministry of Health, Labor, and Welfare, Japan.

REFERENCES

1 Serfaty L, Aumaitre H, Chazouilleres O *et al.* Determinants of outcome of compensated hepatitis C virus-related cirrhosis. *Hepatology* 1998; **27**: 1435–40.
2 Benvegnu L, Gios M, Boccato S, Alberti A. Natural history of compensated viral cirrhosis: a prospective study on the incidence and hierarchy of major complications. *Gut* 2004; **53**: 744–9.
3 Dienstag JL. The role of liver biopsy in chronic hepatitis C. *Hepatology* 2002; **36**: S152–60.
4 Gebo KA, Herlong HF, Torbenson MS *et al.* Role of liver biopsy in management of chronic hepatitis C: a systematic review. *Hepatology* 2002; **36**: S161–72.
5 Namiki I, Nishiguchi S, Hino K *et al.* Management of hepatitis C; Report of the Consensus Meeting at the 45th Annual Meeting of the Japan Society of Hepatology (2009). *Hepatol Res* 2010; **40**: 347–68.
6 Bedossa P, Dargere D, Paradis V. Sampling variability of liver fibrosis in chronic hepatitis C. *Hepatology* 2003; **38**: 1449–57.
7 Intraobserver and interobserver variations in liver biopsy interpretation in patients with chronic hepatitis C. The French METAVIR Cooperative Study Group. *Hepatology* 1994; **20**: 15–20.
8 Sandrin L, Fourquet B, Hasquenoph JM *et al.* Transient elastography: a new noninvasive method for assessment of hepatic fibrosis. *Ultrasound Med Biol* 2003; **29**: 1705–13.
9 Friedrich-Rust M, Ong MF, Martens S *et al.* Performance of transient elastography for the staging of liver fibrosis: a meta-analysis. *Gastroenterology* 2008; **134**: 960–74.
10 Friedrich-Rust M, Wunder K, Kriener S *et al.* Liver fibrosis in viral hepatitis: noninvasive assessment with acoustic radiation force impulse imaging versus transient elastography. *Radiology* 2009; **252**: 595–604.
11 Palmeri ML, Wang MH, Rouze NC *et al.* Noninvasive evaluation of hepatic fibrosis using acoustic radiation force-based shear stiffness in patients with nonalcoholic fatty liver disease. *J Hepatol* 2011; **55**: 666–72.
12 Williams AL, Hoofnagle JH. Ratio of serum aspartate to alanine aminotransferase in chronic hepatitis. Relationship to cirrhosis. *Gastroenterology* 1988; **95**: 734–9.
13 Wai CT, Greenson JK, Fontana RJ *et al.* A simple noninvasive index can predict both significant fibrosis and cirrhosis in patients with chronic hepatitis C. *Hepatology* 2003; **38**: 518–26.
14 Lin ZH, Xin YN, Dong QJ *et al.* Performance of the aspartate aminotransferase-to-platelet ratio index for the staging of hepatitis C-related fibrosis: an updated meta-analysis. *Hepatology* 2011; **53**: 726–36.
15 Sterling RK, Lissen E, Clumeck N *et al.* Development of a simple noninvasive index to predict significant fibrosis in patients with HIV/HCV coinfection. *Hepatology* 2006; **43**: 1317–25.
16 Vallet-Pichard A, Mallet V, Nalpas B *et al.* FIB-4: an inexpensive and accurate marker of fibrosis in HCV infection. comparison with liver biopsy and fibrotest. *Hepatology* 2007; **46**: 32–6.
17 Tamaki N, Kurosaki M, Tanaka K *et al.* Noninvasive estimation of fibrosis progression overtime using the FIB-4 index in chronic hepatitis C. *J Viral Hepat* 2013; **20**: 72–6.
18 Friedrich-Rust M, Ong MF, Herrmann E *et al.* Real-time elastography for noninvasive assessment of liver fibrosis in chronic viral hepatitis. *AJR Am J Roentgenol* 2007; **188**: 758–64.
19 Morikawa H, Fukuda K, Kobayashi S *et al.* Real-time tissue elastography as a tool for the noninvasive assessment of liver stiffness in patients with chronic hepatitis C. *J Gastroenterol* 2011; **46**: 350–8.
20 Koizumi Y, Hirooka M, Kisaka Y *et al.* Liver fibrosis in patients with chronic hepatitis C: noninvasive diagnosis by means of real-time tissue elastography – establishment of the method for measurement. *Radiology* 2011; **258**: 610–17.

21 Tatsumi C, Kudo M, Ueshima K *et al.* Non-invasive evaluation of hepatic fibrosis for type C chronic hepatitis. *Intervirology* 2010; **53:** 76–81.
22 Tomeno W, Yoneda M, Imajo K *et al.* Evaluation of the Liver Fibrosis Index calculated by using real-time tissue elastography for the non-invasive assessment of liver fibrosis in chronic liver diseases. *Hepatol Res* 2012; **12:** 12023.
23 Bedossa P, Poynard T. An algorithm for the grading of activity in chronic hepatitis C. The METAVIR Cooperative Study Group. *Hepatology* 1996; **24:** 289–93.
24 Castera L, Foucher J, Bernard PH *et al.* Pitfalls of liver stiffness measurement: a 5-year prospective study of 13,369 examinations. *Hepatology* 2010; **51:** 828–35.
25 Fraquelli M, Rigamonti C, Casazza G *et al.* Reproducibility of transient elastography in the evaluation of liver fibrosis in patients with chronic liver disease. *Gut* 2007; **56:** 968–73.
26 Arena U, Vizzutti F, Abraldes JG *et al.* Reliability of transient elastography for the diagnosis of advanced fibrosis in chronic hepatitis C. *Gut* 2008; **57:** 1288–93.
27 Rizzo L, Calvaruso V, Cacopardo B *et al.* Comparison of transient elastography and acoustic radiation force impulse for non-invasive staging of liver fibrosis in patients with chronic hepatitis C. *Am J Gastroenterol* 2011; **106:** 2112–20.
28 Colombo S, Buonocore M, Del Poggio A *et al.* Head-to-head comparison of transient elastography (TE), real-time tissue elastography (RTE), and acoustic radiation force impulse (ARFI) imaging in the diagnosis of liver fibrosis. *J Gastroenterol* 2012; **47:** 461–9.
29 Ferraioli G, Tinelli C, Dal Bello B, Zicchetti M, Filice G, Filice C. Accuracy of real-time shear wave elastography for assessing liver fibrosis in chronic hepatitis C: a pilot study. *Hepatology* 2012; **56:** 2125–33.

Hepatology Research

Hepatology Research 2014; 44 (Suppl. 1): 59–70 doi: 10.1111/hepr.12272

Special Report

JSH Guidelines for the Management of Hepatitis C Virus Infection: A 2014 Update for Genotype 1

Drafting Committee for Hepatitis Management Guidelines, the Japan Society of Hepatology*,**

1. INTRODUCTION

RECENTLY, THE MANAGEMENT of chronic hepatitis C virus (HCV) has been greatly advanced with introduction of direct-acting antiviral agents (DAAs) in clinical setting. In Japan, the first DAA, telaprevir (TVR), was approved for patients with chronic hepatitis C in 2011. Along with this, the Japan Society of Hepatology (JSH) produced the first clinical practice guideline for the management of HCV infection, "Guidelines for the Management of Hepatitis C Virus Infection" in May 2012 (English version, 2013[1]). It is our great pleasure that these Guidelines were welcomed and utilized by physicians and other health care providers in daily clinical practices in Japan.

Meanwhile, in September 2013, a second-generation DAA, simeprevir (SMV), was approved for use in Japan. According to Phase III trials in Japan and overseas, SMV has a robust therapeutic effect with better safety profiles compared to TVR. As a result, we have decided to update the clinical guidelines for HCV with launch of this new DAA. SMV has now been approved for use in patients with chronic hepatitis C with genotype 1 and high viral load, and therefore these current Guidelines are updated for patients in this group.

As stated in the previous Guidelines, this is a field that changes rapidly with the accumulation of new evidence, and evidence levels are not shown in the recommendations. At present, several other therapeutic agents are expected to be approved for daily use and we plan to revise these guidelines at appropriate intervals, as new evidence comes to hand.

2. SIMEPREVIR (SMV)

INHIBITORS OF HEPATITIS C virus (HCV) NS3-4A protease are classified into 2 groups on the basis of their molecular structures, linear inhibitors with no branches and macrocyclic inhibitors containing macrocycles. Macrocyclic small molecule compounds show superior affinity and selectivity for therapeutic target proteins.[2] Whereas TVR is a first-generation protease inhibitor with linear structure, SMV is a second-generation protease inhibitor with macrocyclic structure discovered during the optimization process for early protease inhibitors.[3] In vitro resistance testing has yielded different drug resistance profiles, due to their different structures, with cross resistance to SMV seen in TVR resistant mutations at amino acids 155 and 156, whereas mutations at amino acids 36, 54 and 170 were sensitive to SMV, and mutations at amino acids 80 and

**Drafting Committee for Hepatitis Management Guidelines (in alphabetical order):* Yasuhiro Asahina, Department of Gastroenterology and Hepatology, Department for Hepatitis Control, Tokyo Medical and Dental University; Norio Hayashi, Kansai Rosai Hospital; Naoki Hiramatsu, Department of Gastroenterology and Hepatology, Osaka University Graduate School of Medicine; Namiki Izumi, Division of Gastroenterology and Hepatology, Musashino Red Cross Hospital; ‡Kazuhiko Koike, Department of Gastroenterology, Graduate School of Medicine, The University of Tokyo; Hiromitsu Kumada, Department of Hepatology, Toranomon Hospital; Masayuki Kurosaki, Division of Gastroenterology and Hepatology, Musashino Red Cross Hospital; Makoto Oketani, Digestive and Lifestyle-related Diseases, Kagoshima University Graduate School of Medical and Dental Sciences; Fumitaka Suzuki, Department of Hepatology, Toranomon Hospital; †Hajime Takikawa, Department of Medicine, Teikyo University School of Medicine; Atsushi Tanaka, Department of Medicine, Teikyo University School of Medicine; Eiji Tanaka, Department of Medicine, Shinshu University School of Medicine; Yasuhito Tanaka, Department of Clinical Molecular Informative Medicine, Nagoya City University Medical School Graduate School of Sciences; Hirohito Tsubouchi, Kagoshima City Hospital; Hiroshi Yotsuyanagi, Department of Internal Medicine, Graduate School of Medicine, The University of Tokyo (†Chairman, ‡Special Committee Member).

***Correspondence: Atsushi Tanaka, Department of Medicine, Teikyo University School of Medicine, 2-11-1, Kaga, Itabashi-ku, Tokyo 173-8605, Japan. Email: a-tanaka@med.teikyo-u.ac.jp*

168 resistant to SMV alone.[4] Pharmacokinetic studies have shown that once daily administration of SMV provides effective plasma levels 24 h post-dose.[5] SMV shows inhibitory activity against HCV genotypes 1, 2, 4, 5 and 6, with particularly strong anti-proliferative action against genotypes 1a and 1b. In September 2013, the use of SMV in clinical setting was approved in combination with Peg-IFN + RBV in patients with chronic hepatitis C with genotype 1 and a high viral load (≥5.0 log IU/mL).

2.1 Therapeutic results

Phase II trials of SMV + Peg-IFN + RBV combination therapy for genotype 1 chronic hepatitis C include the Japanese DRAGON study (treatment-naïve patients),[6] and the overseas PILLAR study (treatment-naïve patients)[7] and the ASPIRE trial (relapsers following previous treatment and non-responders to previous treatment).[8] Based on the results of these studies, the SMV dosage was set at 100 mg once daily for clinical phase III studies in Japan, and 150 mg once daily for overseas studies. Published Japanese clinical phase III studies comprise the CONCERTO-1 (treatment-naïve patients),[9] CONCERTO-2 (non-responders to previous treatment),[10] CONCERTO-3 (relapsers following previous treatment),[10] and CONCERTO-4 (treatment-naïve patients, non-responders, and relapsers) trials.[11] Published overseas clinical phase III studies comprise the QUEST-1 (treatment-naïve patients),[12] QUEST-2 (treatment-naïve patients),[13] and PROMISE (relapsers) studies.[14] The subjects for the Japanese clinical trials were patients with chronic hepatitis C (excluding cirrhosis) with genotype 1 and a high viral load (≥5.0 log IU/mL), aged 20–70 years (Table 1).

2.1.1 Treatment-naïve patients

The protocol for the Japanese CONCERTO-1 trial,[9] conducted with IFN-naïve subjects, administered SMV 100 mg once daily + Peg-IFNα-2a + RBV triple therapy for the first 12 weeks, then Peg-IFNα-2a + RBV dual therapy for 12 or 36 weeks according to the response-guided therapy (RGT). Using this RGT, subjects with HCV RNA < 1.2 log IU/mL or undetectable after 4 weeks' treatment, and undetectable after 12 weeks, were administered Peg-IFNα-2a + RBV for 12 weeks (total treatment duration 24 weeks), and all other subjects for 36 weeks (total treatment duration 48 weeks). As a result, 99% of subjects met the response-guided criteria, and underwent 24 weeks of treatment. The SVR24 rate was 89% (109/123) for the triple therapy group, significantly higher than that of 57% (34/60) in the control group (Fig. 1).

Peg-IFNα-2b was used in the CONCERTO-4 trial,[11] conducted with IFN-naïve subjects, the same response-

Table 1A Characteristics of patients enrolled in CONCERTO-1/2/3

	Treatment-naïve		*Non-responders*		*Relapsers*
	SMV 12W	PBO	SMV 12W	SMV 24W	SMV 12W
	(n = 123)	(n = 60)	(n = 53)	(n = 53)	(n = 49)
male, %	31.7	40.0	50.9	49.1	40.8
age *	56 (23–69)	54.5 (30–69)	60 (30–70)	60 (24–70)	61 (22–70)
≥65, %	17.9	16.7	26.4	22.6	24.5
BMI, kg/m^2 *	22.0 (16.9–32.9)	22.5 (17.3–33.2)	22.3 (16.8–29.5)	21.9 (19.2–33.4)	22.3 (17.9–32.2)
IL28B SNP (rs8099917), %					
TT	61.7	70	15.1	11.3	71.4
TG	31.7	28.3	83	86.8	28.6
GG	1.6	1.7	1.9	1.9	0
HCV genotype 1b, %	98.4	98.3	100	94.3	98
HCV RNA at baseline, LogIU/mL *	6.3 (4.5–7.2)	6.4 (3.3–7.4)	6.4 (4.6–7.3)	6.4 (5.1–7.0)	6.5 (5.0–7.0)
previous IFN Tx					
IFN mono			7.5	3.8	4.1
IFN+RBV			7.5	7.5	8.2
Peg-IFN mono			0	1.9	4.1
Peg-IFN+RBV			84.9	86.8	83.7

* expressed as median (range).

Table 1B Characteristics of patients enrolled in CONCERTO-4

	Treatment-naïve	*Non-responders*	*Relapsers*
	SMV 12W	SMV 12W	SMV 12W, PR 48W
	(n = 24)	(n = 29)	(n = 26)
male, %	33.3	55.2	50
age *	60 (37–68)	60 (38–70)	53 (45–69)
≥65, %	20.8	31	15.4
BMI, kg/m^2 *	23.0 (18.1–30.2)	22.5 (18.1–31.9)	22.4 (16.9–34.3)
IL28B SNP (rs8099917), %			
TT	66.7	89.7	7.7
TG	33.3	10.3	80.8
GG	0	0	11.5
HCV genotype 1b, %	100	100	96.2
HCV RNA at baseline, LogIU/mL *	6.6 (5.4–7.0)	6.6 (4.9–7.4)	6.5 (5.1–7.4)
previous IFN Tx			
IFN mono		3.4	0
IFN+RBV		0	11.5
Peg-IFN mono		0	0
Peg-IFN+RBV		96.6	88.5

* expressed as median (range).

guided criteria were set, all subjects met the criteria and underwent 24 weeks of treatment, yielding an SVR24 rate of 92% (22/24) (Fig. 2).

In the overseas QUEST-1 study,[12] subjects were administered SMV 150 mg once daily + Peg-IFNα-2a + RBV triple therapy for the first 12 weeks, then response-guided criteria were set as for the CONCERTO-1 trial, with 85% of subjects meeting the criteria and undergoing 24 weeks of treatment. The overall SVR12 rate was 80%; 71% (105/147) in genotype 1a and 90% (105/117) in genotype 1b. The QUEST-2 study[13] set two groups, with either Peg-IFNα-2a or Peg-IFNα-2b, otherwise following the same

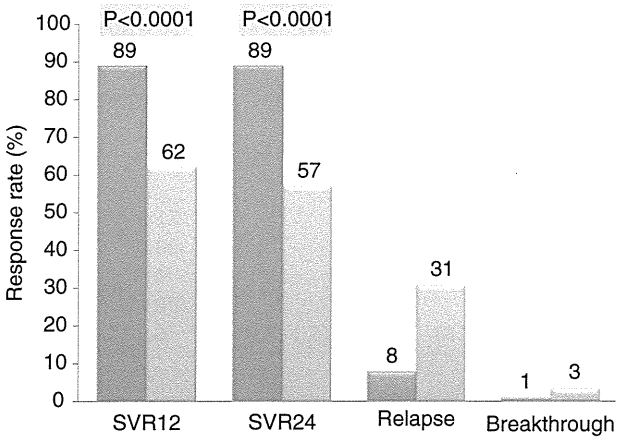

Figure 1 Therapeutic results for SMV + Peg-IFNα-2a + RBV triple therapy for treatment-naïve patients (from CONCERTO-1 trial[9]). ■, SMV + Peg-IFNα-2a + RBV; ■, Peg-IFNα-2a + RBV.

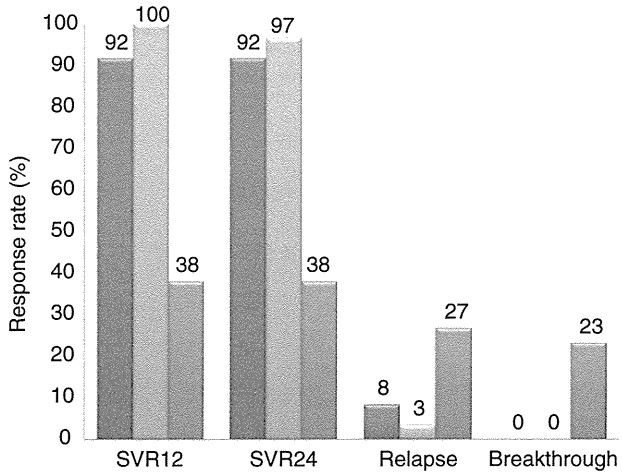

Figure 2 Therapeutic results for SMV + Peg-IFNα-2b + RBV triple therapy for treatment-naïve patients, non-responders, and relapsers (from CONCERTO-4 trial[11]). ■, treatment-naïve cases; ■, relapsers; ■, non-responders. Total treatment duration was 24W for treatment-naive and relapsers, and 48W for non-responders.

protocol as the QUEST-1 study for treatment durations. As a result, 91% of subjects met the criteria and underwent 24 weeks of treatment. The overall SVR12 rate was 81%; 80% (86/107) and 82% (123/150) in genotype 1a and 1b, respectively. The SVR12 rate for Peg-IFNα-2a and Peg-IFNα-2b was 88% and 78%, respectively. In both these studies, triple therapy including SMV yielded significantly higher SVR rates than for 48 weeks of Peg-IFN + RBV dual therapy.

In this way, clinical trials of SMV-based triple therapy regimens were conducted using a response-guided protocol that set a treatment duration of 24 or 48 weeks, with almost all subjects meeting the criteria for the shorter duration. The SVR rate for IFN-naïve subjects in the Japanese studies was 89–92%, and in the overseas studies it was 82–90% for genotype 1b, significantly higher than the SVR rate in the control groups administered 48 weeks of Peg-IFN + RBV dual therapy.

2.1.2 Relapsers following previous treatment

The Japanese CONCERTO-3 trial,[10] conducted with subjects who relapsed following previous IFN therapy, was conducted using a similar protocol to the CONCERTO-1 trial.[9] All subjects met the response-guided criteria and underwent 24 weeks of treatment, yielding an SVR24 rate of 90% (44/49) (Fig. 3). Similarly, the CONCERTO-4 trial,[11] conducted with relapsers, followed a similar therapeutic protocol to the CONCERTO-3 trial,[10] using Peg-IFNα-2b. All subjects met the response-guided criteria and underwent 24 weeks of treatment, yielding an SVR24 rate of 97% (28/29) (Fig. 2).

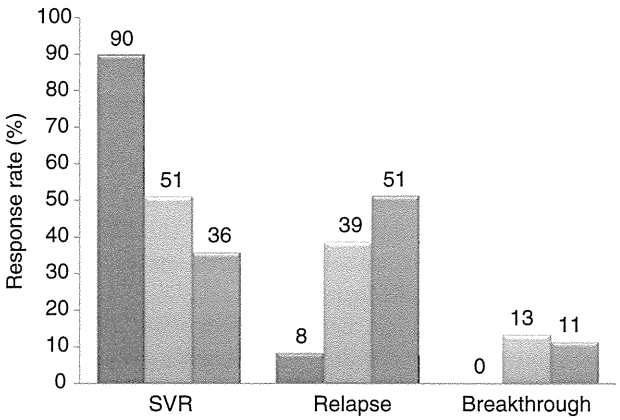

Figure 3 Therapeutic results for SMV + Peg-IFNα-2a + RBV triple therapy for non-responders and relapsers (from CONCERTO-2 and CONCERTO-3 trials[10]). ■, relapsers; ■, non-responders (SMV for 12 wks); ■, non-responders (SMV for 24 wks).

The overseas PROMISE study,[14] conducted with relapsers, was performed using a similar protocol to the QUEST-1 study. As a result, 93% of subjects met the response-guided criteria and underwent 24 weeks of treatment. The overall SVR12 rate was 79%; 70% (78/111) in genotype 1a and 86% (128/149) in genotype 1b.

In this way, in clinical trials of SMV-based triple therapy regimens with relapsers following previous IFN therapy, majority of subjects met the response-guided criteria and underwent 24 weeks of treatment. The SVR rate for the Japanese studies was 90–97%, and in the overseas studies it was 86% for genotype 1b, significantly higher than the SVR rate in the control groups administered 48 weeks of Peg-IFN + RBV dual therapy.

2.1.3 Non-responders to previous treatment

In the Japanese CONCERTO-2 trial,[10] non-responders to previous IFN therapy were administered SMV + Peg-IFNα-2a + RBV triple therapy for 12 weeks (SMV 12W group) or 24 weeks (SMV 24W group). The total treatment duration for both groups was set using response-guided criteria similar to those for the CONCERTO-1 trial,[9] with 96% and 98% of subjects, who completed 24 weeks of treatment respectively, meeting the criteria and finishing the treatment at 24 weeks. The SVR24 rate was 51% (27/53) for the SMV 12W group, and 36% (19/53) for the SMV 24W group (Fig. 3). In the CONCERTO-4 trial,[11] non-responders were administered SMV + Peg-IFNα-2b + RBV triple therapy for 12 weeks, followed by Peg-IFNα-2b + RBV dual therapy for 36 weeks, for a total treatment duration of 48 weeks. The SVR24 rate was 38% (10/26) (Fig. 2).

Although the Japanese CONCERTO-2[10] and CONCERTO-4[11] trials were conducted with non-responders, they did not conduct any further analyses subdividing non-responders into partial responders, with a decrease in the HCV RNA level by ≥2 log IU/mL at week 12 of the previous treatment, and null responders, with a decrease < 2 log IU/mL. On the other hand, the overseas phase II ASPIRE trial,[8] conducted with relapsers and non-responders, reported therapeutic results separately for partial responders and null responders. This trial assigned subjects to one of 3 groups, all with a total treatment period of 48 weeks. They were administered SMV + Peg-IFNα-2a + RBV triple therapy for 12 weeks or 24 weeks, followed by Peg-IFNα-2a + RBV dual therapy for the remaining time, or triple therapy for the entire 48 weeks. SMV was administered in a daily dosage of either 100 mg or 150 mg. The SVR rate for the SMV 12, 24 and 48 week

Table 2 Drugs contraindicated for co-administration with SMV (reproduced from[16])

Generic name	Trade name
Efavirenz	Stocrin
Rifampicin	Rifadin
Rifabutin	Mycobutin

groups was 70%, 66% and 61%, respectively, at the 100 mg dosage, and 67%, 72% and 80% at the 150 mg dosage, with no difference seen between groups due to treatment duration. The SVR rate in relapsers was 85% for both the 100 mg and 150 mg dosages. On the other hand, the SVR rate for partial responders and null responders was 57% and 46%, respectively, at the 100 mg dosage of SMV, and 75% and 51% at the 150 mg dosage. This indicates that within the non-responders, a higher SVR rate is achieved in partial responders than in null responders. In particular, if we confine the analysis to genotype 1b, common in Japanese patients, the SVR rate for partial responders and null responders was 68% and 56%, respectively, at the 100 mg dosage of SMV, and 88% and 58% at the 150 mg dosage. In genotype 1a, the SVR rate for partial/null responders was 56%/33% at 100 mg and 42%/33% at 150 mg.[8]

Recommendations

- *The SVR rate in IFN-naïve subjects was significantly higher for SMV + Peg-IFN + RBV triple therapy than for Peg-IFN + RBV dual therapy for 48 weeks.*
- *A high SVR rate of 90–97% was achieved with SMV + Peg-IFN + RBV triple therapy in relapsers following previous IFN therapy.*
- *An SVR rate of 36–51% was achieved with SMV + Peg-IFN + RBV triple therapy in non-responders to previous IFN therapy.*
- *In an overseas trial, subanalysis of non-responders to previous IFN therapy showed a higher SVR rate in partial responders than in null responders, although there is no data available regarding Japanese subjects.*

2.2 Adverse reactions

In the CONCERT-1 trial,[9] the treatment completion rate was 92.7%. Only 4.9% of subjects in the triple therapy group discontinued treatment due to adverse events, as against 8.3% of subjects in the Peg-IFNα-2a + RBV dual therapy group, with no significant difference between groups.

Elevated bilirubin levels were seen in 40.7% of subjects administered SMV, but these were mild, transient increases not associated with elevated AST or ALT levels. Bilirubin levels in grade 1 (1.1–1.5 mg/dL) were seen in 25.2%, grade 2 (1.6–2.5 mg/dL) in 14.6%, and grade 3 (2.6–5.0 mg/dL) in 0.8%, with no cases of grade 4 (> 5.0 mg/dL). Elevated bilirubin levels are reported to be caused by inhibition of hepatic transporter activity by SMV.[15]

The type and incidence of adverse reactions, including anemia, skin conditions, renal dysfunction, hyperuricemia, malaise, and gastrointestinal symptoms, were similar for SMV + Peg-IFN + RBV triple therapy and for Peg-IFN + RBV dual therapy. The incidence and degree of anemia was similar for both treatment groups; for the SMV-based triple therapy group, the lowest hemoglobin level was ≥10.6 g/dL in 29.3% of subjects, grade 1 anemia (Hb 9.5–10.5 g/dL) in 41.5%, grade 2 anemia (8.0–9.4 g/dL) in 29.3%, and no cases of grade 3 anemia (<8.0 g/dL).

Skin conditions were reported in 57.7% of subjects, all grade 1 or 2, with similar incidences, degrees of severity, and discontinuation rates in the two treatment groups. No serious cutaneous reactions, such as Stevens-Johnson syndrome (SJS) or drug-induced hypersensitivity syndrome (DIHS), were reported.

Recommendations

- *A transient, mild elevation in bilirubin levels may be seen in patients undergoing SMV + Peg-IFN + RBV triple therapy, caused by inhibition of hepatic transporter activity.*
- *The type and incidence of other adverse reactions are similar to those seen with Peg-IFN + RBV dual therapy, yielding high completion rates.*

2.3 Drug interactions

Since SMV is mainly metabolized by CYP3A, co-administration with inhibitors or inducers of CYP3A may affect plasma levels of SMV. In particular, co-administration with strong inducers of CYP3A may enhance the metabolism and markedly lower plasma SMV levels, resulting in attenuating the therapeutic effects. As a result, co-administration of drugs listed in Table 1 is contraindicated.[16]

In addition, since SMV inhibits OATP1B1 and P-glycoprotein, co-administration with drugs transported through these channels may reduce plasma levels of those drugs. The package insert should be referred to before administrating SMV.

Recommendations

- *Since SMV is mainly metabolized by CYP3A and inhibits OATP1A1 and P-glycoprotein, co-administration of*